Thai Environmental Engineering Journal Vol. 37 No. 1 (2023) : 23-32
www.eeat.or.th

Performance of Synthetic Urine-Fed Microbial Fuel Cell at Various Substrate Concentrations and Flow Rates

Warista Chumroen and Petch Pengchai*

Environmental Engineering Laboratory, Circular Resources and Environmental Protection Technology Research Unit (CREPT), Faculty of engineering, Mahasarakham University, Mahasarakham 44150, Thailand
*E-mail : petch.p@msu.ac.th

Abstract

The purpose of this study was to evaluate the performance of microbial fuel cells (MFCs) fed with urine at various substrate concentrations and flow rates. In this work, 3 MFCs were used to process synthetic human urine (SU-D0) and diluted synthetic human urine (SU-D1) at flow rates of 20 L/d (MFC1, HRT=6h), 30 L/d (MFC2, HRT=4h), and 40 L/d (MFC3, HRT=3h). The results showed that MFC2 was the best energy producer (1.221±1.579 mW/m^2 for SU-D0, 0.153 ±0.133 mW/m^2 for SU-D1) and the best nutrient remover due to its maximum removal efficiencies in both SU–D0 (45.6±2.8% for NO_3^-, 41.2±20.0% for NO_2^-, 40.6±12.8% for TN, 36.1±27.7% for PO_4^{3-}) and SU-D1 (39.0±32.4% for NO_3^-, 31.4±10.3% for PO_4^{3-}) conditions. The modified Lineweaver-Burk plot with the determination coefficient (R2) of 0.922-0.975 revealed that the increased substrate loading rate contributed to the higher nutrient removal rate. Furthermore, this study found that the power densities and the removal efficiencies of NO_3^-, NO_2^-, and PO_4^{3-} were positively correlated.

Keywords : Synthetic urine; Microbial fuel cel; Nutrient; Chemical oxygen demand; Removal rate; Power density

Introduction

Human urine mostly comprises 93-96% of water and 4-7% of urea, inorganic salts (chloride, potassium, sodium), ammonia, creatinine, organic acids, and numerous toxins and hemoglobin breakdown products [1]. Udert et al. observed that fresh urine contained 9,200 mg/L total nitrogen, 480 mg/L total ammonia nitrogen, 740 mg/L phosphate, and 10,000 mg/L chemical oxygen demand (COD) [1]. Eighty percent of the nitrogen and fifty of the phosphorus load that enter wastewater treatment facilities come from urine [2], which should be thoroughly removed from wastewater before being discharged into a water source. In Thailand, human waste such as urine and feces is often collected and processed in septic tanks before being released into the ground or wastewater pipelines. Septic tanks can be drained by a municipal service when they are full by pumping the septage out and transferring it to the municipal area's prepared pond. Since source-separated urine can lower the operating costs of wastewater treatment plants (WWTPs) and also help to improve the effluent quality of WWTPs, different European groups began exploring the concept in the 1990s to improve the sustainability of wastewater management [3]. Although human urine in Thailand was not immediately released to wastewater treatment plants or surface water in the environment, it is still better if the nitrogen and phosphorus can be recovered and used at source points. If the human urine was processed independently utilizing microbial fuel cell (MFC) technology, there is also additional benefit, notably ability to harvest electrical energy.

Ieropoulos et al. published the first publications introducing the use of human urine as substrate in MFC systems in 2012 [4]. The benefit of utilizing urine as a substrate for MFCs was shown in this experiment, which ran for more than 11 years [4]. Up to present, it has been proved that MFC-systems fueled by urine can power the low-power equipments such as telecommunication devices [5], LED-lighting systems [6], microcomputers [7] and smart phones [5].

In terms of nutrient removal, the natural transformation of nitrogen and phosphorus-containing compounds during urine hydrolysis was critical. The majority of the nitrogen in fresh urine is urea [1]. During the hydrolysis reaction, $NH_2(CO)NH_2 + 2H_2O \rightarrow NH_3 + NH_4^+ + HCO_3$, urea is broken down to ammonia/ammonium [1]. During this reaction, the pH shifts to more alkaline values between 8.5 and 9.5 [8,] resulting in an increase in ammonia concentration [1]. Because ammonia is volatile, it can easily escape into the atmosphere [1]. Another form of nitrogen in stored urine is struvite ($MgNH_4PO_4 \cdot 6H_2O$) and hydroxyapatite (HAP, $Ca_5(PO_4)_3(OH)$) [9-10] which can deposit at the bottom of the reactor. These processes lower the nitrogen concentration in the urine. In terms of phosphorus removal, 95-100% of phosphorus in fresh urine is in soluble phosphate form [11]. When the pH of the solution rises due to urea hydrolysis, 30-40% of the dissolved phosphorus precipitates as struvite or hydroxyapatite [1, 12-13]. Santoro et al. studied urine-fed microbial fuel cells [1]. The results showed that urea hydrolysis increased ammonium ion concentrations fourfold, while sulfate and phosphorous concentrations decreased due to significant reductions in calcium and magnesium levels [1]. Struvite, potassium struvite, and hydroxyapatite were discovered in the precipitate on the bottom of MFC reactors [1].

Despite the fact that MFC has been demonstrated by numerous groups of researchers to be one of the most effective nutrient removal technologies capable of producing electrical energy during urine treatment, the application of urine-fed MFC in Thailand is not widely pursued. Therefore, this study was planned to provide information on the performance of urine-fed MFCs in terms of both nutrient removal and energy production. In this study, Thai human urine was used as the substrate during the inoculum period, while synthetic human urine was used as the influent during the treatment period.

In a number of MFC studies, flow rate and substrate concentration are major parameters influencing MFC performance. Potrykus et al., for example, observed that increasing the MFC influent flow rate resulted in greater COD removal rates of up to 396 g/(L/d) and higher electric power output of nearly 18 mW/m^2 [14]. Ni et al. had found that the concentration of a selected substrate is positively correlated with the output voltage of MFC and COD removal rate [15]. In order to better understand how urine-fed MFCs function, this study was conducted with the primary goal of evaluating the performance of urine-fed MFCs at various substrate concentrations and flow rates. Higher flow rates and greater substrate concentrations, according to our hypothesis, might lead to increased removal rates and power output. The findings of this study should assist in the development and application of urine-fed MFCs in Thailand.

Materials and Methods

Construction of the MFC systems

As depicted in Figure 1, the authors constructed 3 upflow MFCs. A 10-cm-diameter, 85.4-cm-long PVC (polyethylene) pipe was used to create the anode chamber of each MFC. The anode chamber's media bed, which has a height of 50 cm and a void ratio of 75%, and a total pore volume of 5 L, was built using 1,575 bundles of nylon strands (1.6 mm in diameter, 10 cm long). Each MFC's upper portion has a cathode compartment built on it by joining a 35.4-cm-long PVC reducer junction to the top of the anode chamber without any partitions (Adapted from the work of Sukkasem et al. [16]). The anode chamber was constructed with an outlet port at the top and an inlet port at the bottom. Before being employed as the electrodes, graphite plates (Kimtech Technology Ltd., Part.) underwent pretreatment by being heated at 450 ºC for 30 minutes [17]. The media bed of each anode chamber was equipped with a triangular

graphite plate (20.77 cm^2) acting as an anode. On the water's surface of each outlet port, an ellipse-shaped graphite plate (20.79 cm^2) was positioned as an air cathode.

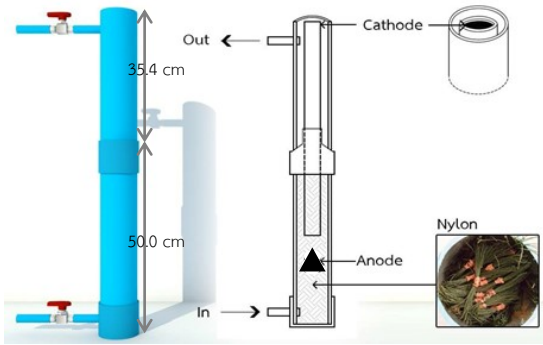

Figure 1 The synthetic urine-fed MFC

Inoculation for Experimental setup

Real human urine was combined in a 1:10 volume ratio with activated sludge collected from the Mahasarakham hospital wastewater treatment plant and stirred for 6 hours. The mixture's supernatant was used as the inoculum after being left in the mixture for 30 minutes. Synthetic urine contained 0.651 g/L of $CaCl_2 \cdot H_2O$, 0.651 g/L of $MgCl_2 \cdot 6H_2O$, 4.6 g/L of NaCl, 2.3 g/L Na_2SO_4, 0.65 g/L of Sodium citrate, 0.02 g/L of Sodium oxalate, 2.8 g/L of KH_2PO_4, 1.6 g/L of KCl, 1.0 g/L of NH_4Cl, 25 g/L of Urea, 1.1 g/L of Creatine, and 10 g/L of Tryptic soy broth [18]. Each MFC was loaded with 12-L inoculum, and the substrate—a combination of 30-L genuine human urine and 90-L synthetic urine—was pumped into each anode compartment. The desired influent flow rates were generated by combining DC dosing pumps (maximum flow rate = 4 L/min, 6.8 bar, 12 V, 3 A, Chao Pra Ya Karn Kaset Co. Ltd) with DC voltage control devices (Chao Pra Ya Karn Kaset Co. Ltd) to reduce the pump power and applying multiple PVC tubes into the feeding lines to create hydraulic resistance. With flow rates of 20 L/d for MFC1 (6-h hydraulic retention time [HRT]), 30 L/d for MFC2 (4-h HRT), and 40 L/d for MFC3 (3-h HRT), the substrate was continuously delivered to the 3 reactors (100 % recycle) for two weeks. The HRTs in this study were calculated based on void volume and flow rate (HRT = void volume/flow rate). Using a multimeter (GW INSTEK Model: GDM - 8255A), electrical voltages (OCVs: open circuit voltages) between the cathode and anode of each MFC were monitored in real time. After the inoculation, each MFC underwent a polarization experiment to determine the suitable external resistor for the MFC system's operation.

MFC System operation

The treatment of synthetic urine by MFC systems was mostly done in a closed electrical circuit in which a cathode and an anode of each MFC were connected to the external resistor defined in the polarization experiment. During the first phase of the treatment, each MFC was fed synthetic urine (SU-D0) continuously for 11 days. Concentrations of COD, NO_3, NO_2, TAN, TN, and PO_4 in SU-D0 were 3,078.8 ± 83.3 mgCOD/L, 2.0 ± 0.2 mgNO_3-N/L, 4.2 ± 1.4 mgNO_2-N/L, 31.4 ± 6.9mgTAN-N/L, 53.8 ± 7.6mgTN/L, and 369 ± 174 mgPO_4-P/L, respectively. The MFCs were operated in open circuit mode for the first 129 hours. At the end of 129 hours, the polarization experiment was performed to select suitable external resistors for the MFCs. The MFCs were then connected to the selected external resistors and performed in a closed electrical circuit from the 130^{th} to 334^{th} h. In the second phase, new suitable external resistors were determined by the second polarization experiment and equipped in the MFCs. The MFCs were then fed continuously for 19 days with diluted synthetic urine (SU-D1, synthetic urine: tap water = 1:1 by volume). Concentrations of COD, NO_3, NO_2, TAN, TN, and PO_4 in SU-D1 were 1,919.1 ± 527.2 mgCOD/L, 1.2 ± 0.7 mgNO_3-N/L, 6.3 ± 1.2 mgNO_2-N/L, 1.8 ± 0.4 mgTAN-N/L, 12.4 ± 3.5mgTN/L, and 27.4 ± 3.0 mgPO_4-P/L, respectively. The flow rates used in both the SU-D0 and SU-D1 treatment periods were the same as those used in the inoculation period, i.e. 20 L/d for MFC1, 30 L/d for MFC2, and 40 L/d for MFC3. Throughout the operation period, influent and effluent samples from each reactor were collected and analyzed for water quality. The multimeter was used to measure the electrical voltage drops across the resistor at each MFC (CCVs: closed circuit voltages).

Polarization test

In this study, a polarization test was performed to determine the external resistor that resulted in the maximum power output for each MFC system. The MFC circuit was closed by connecting an external resistor to a cathode and an anode. CCV values across the resistor were measured for 5 minutes before replacing the current external resistor with a new external resistor with a different resistance value. In the test, the resistance value of an external resistor (R_{ex}) was changed from 51 to 10,000 ohms. The MFC power output (P) was then calculated based on the CCV and R_{ex} values derived from equation (1). The R_{ex} that resulted in the highest P for each MFC system was defined as the suitable R_{ex} and was chosen to be used in the system during wastewater treatment.

$$P = CCV/ R_{ex}^2 \quad (1)$$

Analytical methods and calculation

The following methods were used to analyze water samples: closed reflux, titrimetric method [19] for COD, phenol disulphonic acid method for nitrate (NO_3^-) [20], colorimetric method for nitrite (NO_2^-) [19], closed reflux, nesslerization method for total ammonia ion (TAN) [19, 21], Spectrophotometry using phenol after alkaline peroxodisulfate digestion method for total nitrogen (TN) [22], vanadomolybdophosphoric acid method for phosphate (PO_4^{3-}) [19]. Dissolved oxygen (DO), pH, and oxidation-reduction potential (ORP) were measured using the meters. Wastewater treatment capability was considered from removal efficiencies ($Efficiency_{removal}$) and removal rate ($Rate_{removal}$) shown in equation (2) and (3). C_0 is a pollutant concentration of the influent and C is a pollutant concentration of the effluent. The average value of parameters such as $Efficiency_{removal}$, $Rate_{removal}$, C, and so on was shown with the standard deviation in the form of average value ± standard deviation of the data.

$$Efficiency_{removal} = (C_0\text{-}C)\times 100/C_0 \quad (2)$$

$$Rate_{removal} = (C_0\text{-}C)/HRT \quad (3)$$

For the kinetic analysis of the removal performance, the experimental data were plotted in a modified Lineweaver-Burk model based on the Michaelis-Menten kinetics equation (equation (4) [23]), where Q is the flow rate (L/d), and V is the total volume of the MFC. The regression analysis of the plot defined two constants: U_{max} (the possible maximum removal rate (mg/L·h)), and K_{m*} (the modified Michaelis-Menten saturation constant (mg/L)).

$$V/Q(C_0\text{-}C) = (K_{m*}/U_{max})\ (V/QC_0) + (1/ U_{max}) \quad (4)$$

The external resistor resistance (R_{ex}) and CCV values measured during MFC system operation were used to calculate P (see equation (1)) and power density (PD) (see equation (5)) for each MFC. An anode's projected area is referred to as A_{anode}.

$$PD = CCV/ (R_{ex}^2 \cdot A_{anode}) \quad (5)$$

Results and Discussions

Synthetic Urine Treatment Capability

During the SU-D0 and SU-D1 treatment periods, the pH of the influent ranges between 6.07-8.57, while the pH of the MFC1-3 effluent ranges between 8.35-8.86. The alkaline quality of all effluent and most influent samples implied a high concentration of ammonia nitrogen in un-ionized form [24]. ORP values of -54 to 35 mV and -128 to -3 mV were measured inside the anode chamber during the SU-D0 and SU-D1 treatment periods, respectively. Kim et al. proposed 7.0 as the optimal pH and -250 mV as the minimum ORP level for aerobic denitrification [25]. In comparison to the suggested condition [25], this result suggested the possibility of denitrification within the anode chambers.

COD removal was observed in all MFC reactors, as shown in Figure 2. During the SU-D0 treatment period, COD removal efficiencies ranged from 6.3 to 64.3%, with average values of 30.6±25.0%, 36.8±17.4%, and 46.3±13.9% for MFC1, MFC2, and MFC3, respectively. For SU-D1 treatment, the COD removal efficiencies ranged from -28.6 to 76.4% with the average values of 12.5±30.1%, 30.5±16.4%, and 46.1±13.2% for MFC1, MFC2, MFC3, respectively. The negative removal efficiencies were driven by greater

COD concentration in MFC1 effluents on days 3 (1,627 mg/L) and 5 (1,831 mg/L) than in the influent (1,424 mg/L). This outcome might have been produced by the medium's discharge of microbial biofilm on those days. The removal efficiency of MFC3 (HRT = 3h) appeared to be higher than that of the other two reactors (MFC1, HRT = 6h; MFC2, HRT = 4h). This trend, however, was not statistically supported (paired t-test, 0.05 significance level). The fluctuation in influent concentration (Figure 2-7) in both SU-D0 and SU-D1 conditions may be caused by microbial digestion inside each tank and precipitation, particularly precipitation in the form of struvite.

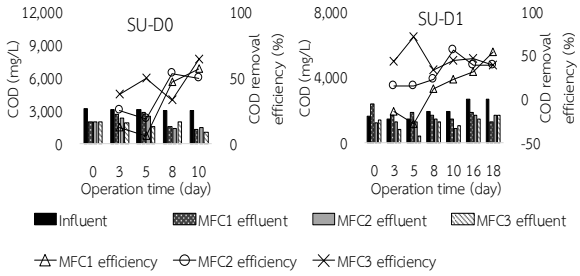

Figure 2 COD removal during the treatment of synthetic urine by MFCs

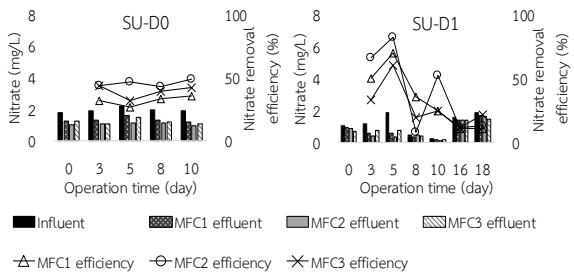

Figure 3 Nitrate and removal during the treatment of synthetic urine by MFCs

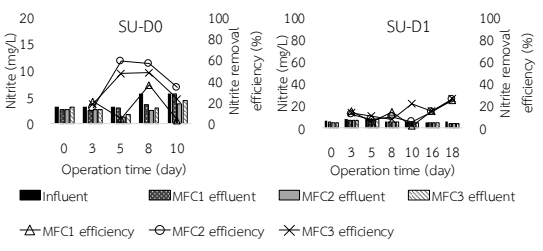

Figure 4 Nitrite removal during the treatment of synthetic urine by MFCs

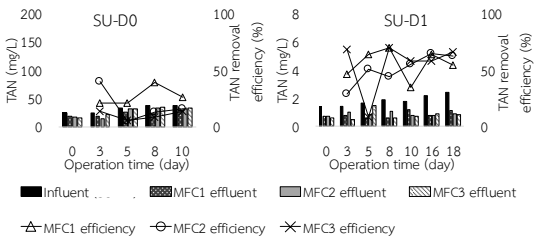

Figure 5 Total amonia nitrogen removal during the treatment of synthetic urine by MFCs

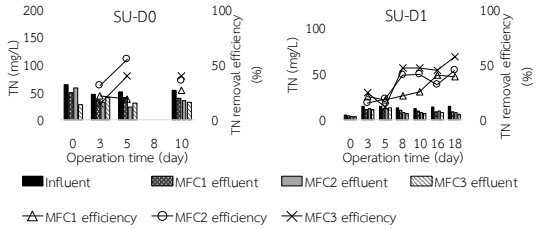

Figure 6 Total nitrogen removal during the treatment of synthetic urine by MFCs

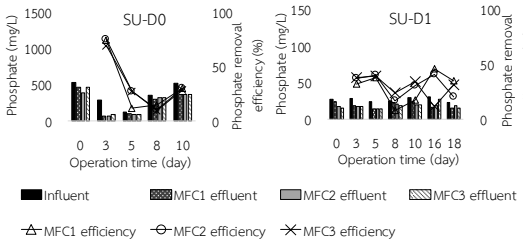

Figure 7 Phosphate removal during the treatment of synthetic urine by MFCs

Concentrations and removal efficiencies of nitrogen compounds and phosphate during the treatment period were shown in Figure 3-7. During SU-D0 treatment period, NO_3^- removal efficiencies ranged from 26.5 to 48.8% with the average values of 32.0±4.0% (MFC1), 45.6±2.8% (MFC2), and 39.2±5.4% (MFC3); NO_2^- removal efficiencies ranged from 3.4 to 58.8% with the average values of 16.5±15.7% (MFC1), 41.2±20.0% (MFC2), and 34.3±15.8% (MFC3); TAN removal efficiencies ranged from 4.9 to 40.2% with the average values of 26.6±8.5% (MFC1), 18.5±15.2% (MFC2), and 10.3±3.9% (MFC3); TN removal efficiencies ranged from 14.6 to 55.1% with the average values of 26.6±8.5% (MFC1), 40.6±12.8% (MFC2), and 31.3±14.4% (MFC3); PO_4^{3-}

removal efficiencies ranged from 10.1 to 75.4% with the average values of 33.2±29.3% (MFC1), 36.1±27.7% (MFC2), and 34.2±25.1% (MFC3).

For SU-D1 treatment, NO_3^- removal efficiencies ranged from 7.7 to 70.2% with the average values of 33.8±23.4% (MFC1), 39.0±32.4% (MFC2), and 28.6±14.4% (MFC3); NO_2^- removal efficiencies ranged from 5.3 to 26.1% with the average values of 12.7±8.4% (MFC1), 12.4±7.1% (MFC2), and 15.9±7.0% (MFC3); TAN removal efficiencies from between 8.2 to 70.0% with the average values of 55.4±13.2% (MFC1), 50.9±13.3% (MFC2), and 54.7±23.3% (MFC3); TN removal efficiencies ranged from 15.0 to 45.0% with the average values of 27.4±9.7% (MFC1), 31.9±12.6% (MFC2), and 38.6±17.0% (MFC3); PO_4^{3-} removal efficiencies ranged from 17.2 to 46.2% with the average values of 29.8±14.1% (MFC1), 31.4±10.3% (MFC2), and 30.2±10.4% (MFC3).

In terms of removal rates, COD and PO_4^{3-} average removal rates increased as influent flow rate (MFC1<MFC2<MFC3) and substrate initial concentration (SU-D1<SU-D0) doubled (see Figure 8). The positive correlation trend between the removal rate and the influent flow rate is consistent with the findings of Mongkulphit et al., who found that higher flow rates resulted in higher pollutant removal rates and higher power densities under linear regression equations with determination coefficients (R^2) of 0.81-0.99 [26].The concordance between increasing substrate initial concentration and increasing removal rate in this study corresponds to the theory of Michaelis-Menten equation [27]. The initial concentration of substrates may provide high enzyme concentration, resulting in high enzyme reaction rates [27]. However, excessive substrate concentrations may cause substrate inhibition, which significantly reduces the hydrolysis rate [28]. This could be one of the reasons why the average removal rates of TAN, NO_3^-, and NO_2^- at SU-D0 were lower than at SU-D1. If the data were individually analyzed in SU-D0 and SU-D1 scenarios, it was discovered that the increase in flow rate caused an increase in the removal rates of NO_3^- and PO_4^{3-}. In the case of low substrate concentration (SU-D1), the TAN removal rate also showed a similar pattern. The previous researches [14, 26] are compatible with this finding as well. The improving mixing condition, which is associated with increasing flow rate, might be the key to higher NO_3^- and PO_4^{3-} removal rates, as well as TAN removal rates under low substrate conditions. Nevertheless, when the flow rate rose, the TAN and NO_2^- removal rates in the SU-D0 condition declined. Sufficient HRT appeared to be the critical factor in achieving high TAN and NO_2^- removal rates in the high substrate condition.

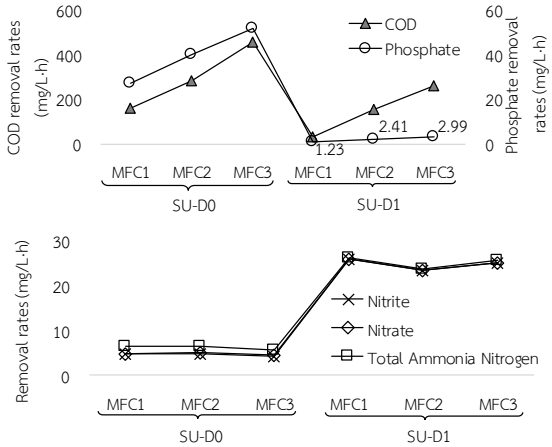

Figure 8 Average removal rates during the treatment of synthetic urine by MFCs

According to MFC literature, nitrogen removal in MFC may occur as a result of 1) the nitrification process at the cathode compartment, in which oxygen gas is used as an electron acceptor in the nitrification process to convert ammonium to nitrite and nitrate, and 2) the electricity generation process, in which both nitrate and nitrite can serve as cathode electron acceptors [29], 3) volatilization of ammonia [30]. Furthermore, the studies indicated that phosphorus could be removed up to 82% by microbial absorption in MFC systems, with 40% recovered by chemical precipitation as struvite at the cathodes [29]. Struvite precipitation [31] is thought to improve electron acceptation at the cathode compartment.

The negative association between NO_2^- and the other pollutants, such as NO_3^-, PO_4^{3-}, and TAN, was revealed by the relationship

between the rates of nutrient removal in Figure 9. Because NO_2^-, NO_3^-, and PO_4^{3-} are cathode electron acceptors and are thought to be largely removed at the cathode surface, they competed with one another. Furthermore, since it was believed that some TAN would be removed through volatilization, a high TAN removal rate would lower the rate at which NO_2^- is produced, which might slow down the process that removes NO_2^-. In order to validate these explanations, additional research is necessary.

Kinetic analysis for COD and nutrient removal

Figure 10 depicts the fitting of our experimental data into the modified Lineweaver-Burk model (= 0.922 and 0.975). The model suggested that a higher substrate loading rate would resulted in a faster removal rate. The equations derived here are helpful in the design of MFCs for treating urine. However, as the components in actual human urine may be 3-4 times greater than those of synthetic urine, further experiments at extremely high substrate concentrations are required before applying the modified Lineweaver-Burk model to develop the human urine treatment process.

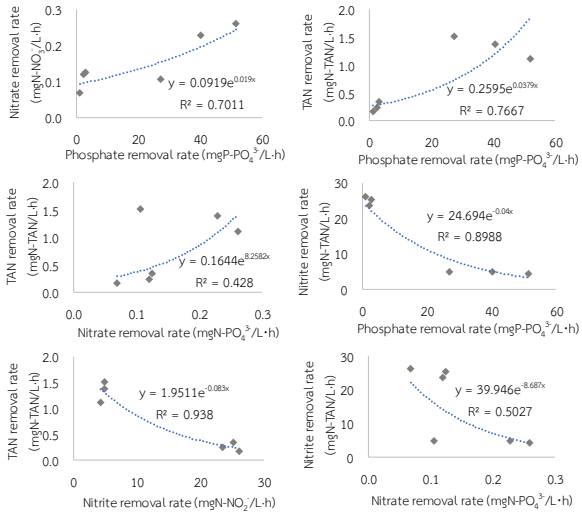

Figure 9 Relationship between average removal rates of each component during the treatment of synthetic urine by MFCs

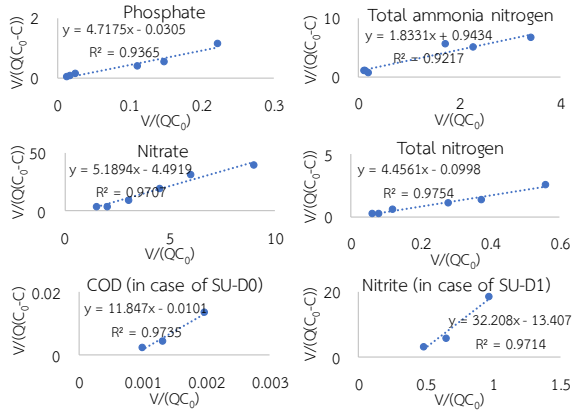

Figure 10 Modified Lineweaver-Burk plot of the synthetic urine treatment using MFCs

Electricity generation Capability

MFCs were operated in an open circuit condition for the first 129 hours of the SU-D0 treatment period. The OCV of 3 MFCs increased from 0.196 to 0.46 V at 24th h to 0.786 to 0.838 V and nearly remained steady from 72nd to 120th h (Figure 11a). A resistor of 10,000 ohms, 1,000 ohms, and 680 ohms was chosen and applied to MFC1, MFC2, and MFC3, respectively, from 130th h to 344th h, based on the results of the first polarization experiment. Throughout the experiment, one side of each resistor was connected to the anode and the other edge to the cathode of each MFC. Figure 11b displays the CCV data obtained during the SU-D0 treatment. The maximum CCV for MFC1 (0.137 V), MFC2 (0.183 V), and MFC3 (0.101 V) appeared at 130th h and 285th h, respectively. In MFC2 and MFC3, the CCV trend was pendulous, whereas in MFC1, it was fairly stable. Due to the suggestion given by the result of the second polarization experiment, 10,000-ohm resistors were added to all MFCs during the SU-D1 treatment period. Figure 11c showed CCV generated by the MFCs during the SU-D1 treatment. When compared to the CCV trends during the SU-D0 treatment period, all MFCs showed considerably lower and more steady trends.

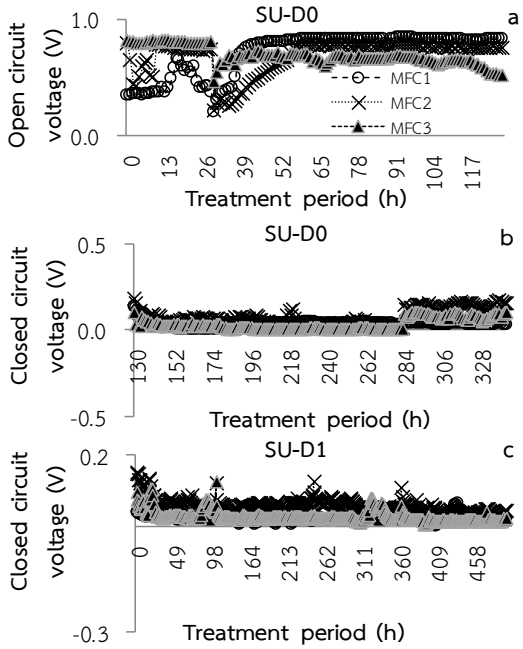

Figure 11 Voltage data collected during the treatment of synthetic urine by MFCs

PD data during the treatment period were displayed in Figure 12. The most powerful generator of electricity was MFC2 (PD = 1.221±1.579 mW/m^2 for SU-D0, 0.153 ±0.133 mW/m^2 for SU-D1), followed by MFC3 (PD = 0.262 ±0.576 mW/m^2 for SU-D0, 0.041 ±0.071 mW/m^2 for SU-D1), and MFC1 (PD = 0.079 ±0.101 mW/m^2 for SU-D0, 0.019 ±0.020 mW/m^2 for SU-D1).

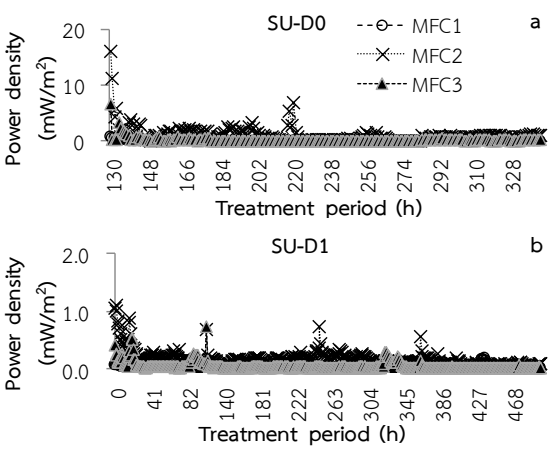

Figure 12 Power density data collected during the treatment of synthetic urine by MFCs

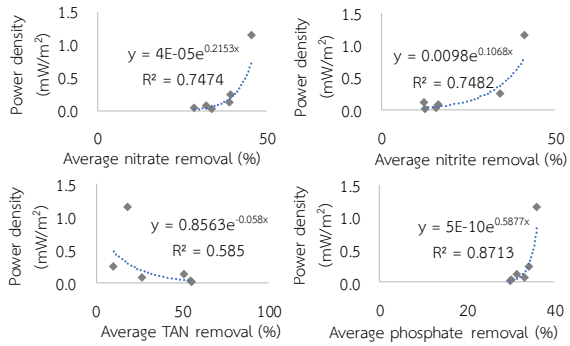

Figure 13 Relationship between power density and removal efficiencies during the treatment of synthetic urine by MFCs

The relationship between PD and the nutrient removal efficiency was explored to provide more understanding. According to the result presented in Figure 13, high power density occurred under the circumstances of high NO_3^-, NO_2^-, and PO_4^{3-} removal efficiencies. One possibility could be that some of their removal processes improved the flow of electrons from the anode to the cathode of MFCs. For instance, NO_3^- and NO_2^- can both serve as cathode electron acceptors [29] and be removed from the influent. Furthermore, electron transport at the cathode surface might be improved by the PO_4^{3-} struvite precipitation reaction [31].

Conclusion

When synthetic human urine was applied to 3 MFCs at 2 levels of substrate concentration and 3 different flow rates, the MFC with the medium level of flow rate (MFC2, 30 L/d, HRT=4h) demonstrated the best performance in both the energy production and nutrient removal aspects. The modified Lineweaver-Burk plot's showed that the substrate loading rate varied in accordance with the nutrient removal rate. As high power density was observed in the condition of high NO_3^-, NO_2^-, and PO_4^{3-} removal efficiencies, the electricity generated by MFCs in this study was considered beneficial for NO_3^-, NO_2^-, and PO_4^{3-}removal.

Acknowledgment

We truly appreciate everyone who has given us the opportunity to perform this research. We were grateful for the insightful guidance provided by Associate Professor Dr. Kanyarat Holasut and Associate Professor Dr. Nattawoot Suwant tota. Finally, we would like to express our gratitude to Mahasarakham University for funding this research project.

References

[1] Santoro, C., Garcia, M.J.S., Walter, X.A., You, J., Theodosiou, P., Gajda, I., Obata, O., Winfield, J., Greenman, J. and Ieropoulos, I. 1995. Urine in Bioelectrochemical Systems: An Overall Review. Chem Electro Chem. 10.1002/celc.201901995. Accessed: May. 18, 2022 [Online]. Available: https://chemistry-europe.onlinelibrary.wiley.com/doi/10.1002/celc.201901995.

[2] Landry, K.A. and Boyer, T.H. 2016. Life Cycle Assessment and Costing of Urine Source Separation: Focus on Nonsteroidal Antiinflammatory Drug Removal. Water Research. 105: 487-495.

[3] You, J., Greenman, J., Melhuish, C. and Ieropoulos, I. 2014. Electricity Generation and Struvite Recovery from Human Urine Using Microbial Fuel Cells. Journal of Chemical Technology and Biotechnology. 91(3): 647-654.

[4] Ieropoulos, I., Greenman, J. and Melhuish, C. 2012. Urine Utilisation by Microbial Fuel Cells; Energy Fuel for The Future. Physical Chemistry Chemical Physics. 14: 94-98.

[5] Walter, X.A., Stinchcombe, A., Greenman, J. and Ieropoulos, I. 2017. Urine Transduction to Usable Energy: A Modular MFC Approach for Smartphone and Remote System Charging. Applied Energy. 192: 575-581.

[6] Walter, X.A., Merino-Jiménez, I., Greenman, J. and Ieropoulos, I. 2018. PEE POWER® urinal II – Urinal Scale-up with Microbial Fuel Cell Scale-down for Improved Lighting. Journal of Power Sources. 392: 150-158.

[7] Walter, X.A., Greenman, J. and Ieropoulos, I. 2020. Microbial Fuel Cells Directly Powering a Microcomputer. Journal of Power Sources. 446: 227328.

[8] Silvester, K.R., Bingham, S.A., Pollock, J.R., Cummings, J.H. and O'Neill, I.K. 1997. Effect of Meat and Resistant Starch on Fecal Excretion of Apparent N-nitroso Compounds and Ammonia from the Human Large Bowel. Nutr. Cancer. 29: 13-23.

[9] Udert, K.M., Larsen, T.A., Biebow, M. and Gujer, W. 2003. Urea Hydrolysis and Precipitation Dynamics in a Urine-Collecting System. Water Research. 37: 2571-2582.

[10] Udert, K.M., Larsen, T.A. and Gujer, W. 2003. Biologically Induced Precipitation in Urine-collecting Systems. Water Sci. Technol. Water Supply. 3(3): 71-78.

[11] Larsen, T.A. and Gujer, W. 1996. Separate Management of Anthropogenic Nutrient Solutions (Human Urine). Water Science and Technology. 34(3-4): 87-94.

[12] Udert, K.M., Larsen, T.A. and Gujer, W. 2003. Estimating the Precipitation Potential in Urine-collecting Systems. Water Research. 37: 2667-2677.

[13] You, J., Greenman, J., Melhuish, C. and Ieropoulos, I. 2016. Electricity Generation and Struvite Recovery from Human Urine Using Microbial Fuel Cells. Journal of Chemical Technology and Biotechnology. 91: 647-654.

[14] Potrykus S., Mateo S., Nieznnski J. and Fernández-Morales F.J. 2020. The Influent Effects of Flow Rate Profile on the Performance of Microbial Fuel Cells Model. Energies. 13(18): 4735.

[15] Ni H., Wang K., Lv S., Wang X., Zhuo L. and Zhang J. 2020. Effects of Concentration Variations on the Performance and Microbial Community in Microbial Fuel Cell Using Swine Wastewater. Energies. 13(9): 2231.

[16] Sukkasem, C., Laehlah, S., Hniman, A., O'thong, S., Boonsawang, P., Rarngnarong, A., Nisoa, M. and Kirdtongmee, P. 2011. Upflow Bio-filter Circuit (UBFC): Biocatalyst Microbial Fuel Cell (MFC) Configuration and Application to Biodiesel Wastewater

Treatment. Bioresource Technology. 102(22): 10363-10370.

[17] Choudhury, P., Uday, U.S., Bandyopadhyay, T.K., Ray R.N. and Bhunia, B. 2017. Performance Improvement of Microbial Fuel Cell (MFC) Using Suitable Electrode and Bioengineered Organisms: A Review. Bioengineered. 8(5): 471-487.

[18] McLean, R.J.C., Nickel, J.C., Cheng, K.-J., Costerton, J.W. and Banwell, J.G. 1988. The Ecology and Pathogenicity of Urease-producing Bacteria in the Urinary Tract. CRC Critical Reviews in Microbiology. 16(1): 37-79. Accessed: Jan. 2, 2023 [Online]. Available: https://scholar.google.com/citations?view_op=view_citation&hl=en&user=qDVk4ZAAAAAJ&cstart=100&pagesize=100&sortby=pubdate&citation_for_view=qDVk4ZAAAAAJ:zYLM7Y9cAGgC.

[19] American Public Health Association (APHA). 2017. Standard Methods for the Examination of Water and Wastewater. American Water Works Association, 22rd ed. Washington D.C., New York.

[20] Kaul, S.N. 2002. Water and Wastewater Analysis. Daya Publishing House, New Delhi.

[21] U.S. Environmental Protection Agency (USEPA). 1993. Method 350.1 Determination of ammonia nitrogen by semi-automated colorimetry. 2nd revision. Environmental Monitoring Systems Laboratory, Office of Research and Development, Ohio.

[22] Gou Y. 2001. Determination of total nitrogen in water samples by spectrophotometry using phenol after alkaline peroxodisulfate digestion. Bunseki Kagaku. 50(7): 481-486.

[23] Dowd, J.E. and Riggs, D.X. 1965. Comparison of Estimates of Michaelis-Menten Kinetic Constants from Various Linear Transformations. The Journal of Biological Chemistry. 240(2): 863-869.

[24] Puyol, D., Carvajal-Arroyo, J M, Li, G.B., Dougless, A., Fuentes-Velasco, M., Sierra-Alvarez, R. and Field, J.A. 2014. Field. High pH (and not Free Ammonia) Is Responsible for Anammox Inhibition in Mildly Alkaline Solutions with Excess of Ammonium. Biotechnology Letters. 36(10): 1981-1986.

[25] Kim, S.H., Song, S.H. and Yoo, Y.J. 2004. The pH as a Control Parameter for Oxidation-Reduction Potential on the Denitrification by Ochrobactrum anthropi SY 509. Journal of Microbiology and Biotechnology. 14(3): 639-642.

[26] Mongkulphit, S., Pengchai, P. and Suwannata N. 2021. Influence of Very High Flow Rates on Performance of Biofilter-Microbial Fuel Cells. International Journal of Environmental Science and Development. 12(3): 69-74.

[27] Robinson, P.K. 2015. Enzymes: principles and biotechnological applications. Essays Biochem. 59: 1-41. Accessed: Jan. 2, 2023 [Online]. Available: https://portlandpress.com/essaysbiochem/article/doi/10.1042/bse0590001/88345/Enzymes-principles-and-biotechnological.

[28] Aslanzadeh, S., Ishola, M., Richards, T. and Taherzadeh, M. 2014. An Overview of Existing Individual Unit Operations. Biorefineries. Integrated Biochemical Processes for Liquid Biofuels. 3-36. Accessed: Jan. 2, 2023 [Online]. Available: https://www.researchgate.net/publication/289707814_An_Overview_of_Existing_Individual_Unit_Operations.

[29] Guo Y., Wang J., Shinde S., Wang X., Li Y., Dai Y., Ren J., Zhang, P. and Liu, X. 2020. Simultaneous Wastewater Treatment and Energy Harvesting in Microbial Fuel Cells: An Update on the Biocatalysts. RSC Advances. 10: 25874-25887.

[30] Paucar, N.E. and Sato, C. 2021. Microbial Fuel Cell for Energy Production, Nutrient Removal and Recovery from Wastewater: A Review. Processes. 9(8): 1318.

[31] Liao, M., Yuan, L., Enling, T., Weiqi, M. and Hong, L. 2020. Phosphorous Removal and High-purity Struvite Recovery from Hydrolyzed Urine with Spontaneous Electricity Production in Mg-air Fuel Cell. Chemical Engineering Journal. 391(1): 123517.